Research Article | Open Access

Complex Engineering Systems

Sun et al. Complex Eng. Syst. 2026, 6, 6 DOI: 10.20517/ces.2025.85

Consensus of heterogeneous second-order nonlinear multi-agent systems via pinning sampling control

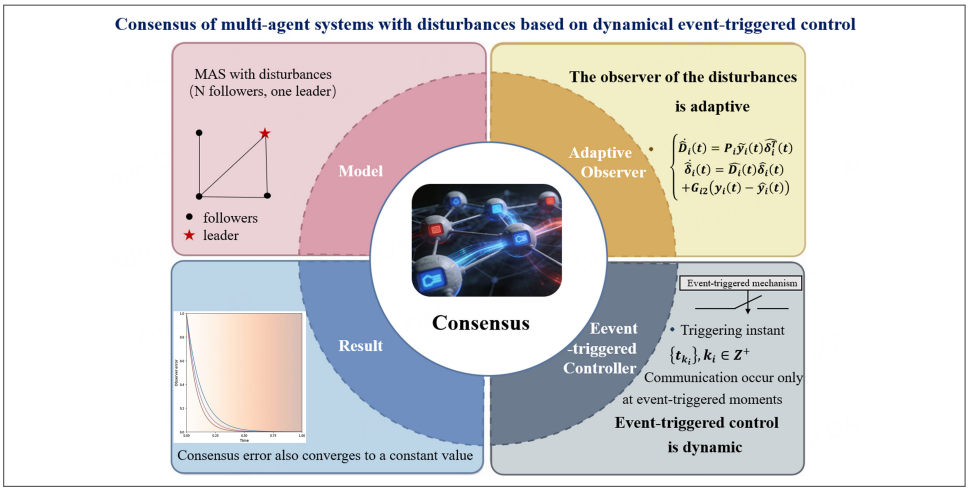
Sijiao Sun[1,2], Zhengxin Wang[2], Chengdai Huang[3], Yuanzhen Feng[2], Min Xiao[4]

Keywords:
Consensus, heterogeneous system, MASs, pinning sampling control, event-triggered control

Citation: Sun, S.; Wang, Z.; Huang, C.; Feng, Y.; Xiao, M. Consensus of heterogeneous second-order nonlinear multi-agent systems via pinning sampling control. *Complex Eng. Syst.* **2026**, *6*, 6. https://dx.doi.org/10.20517/ces.2025.85

Received: 19 Dec 2025
First Decision: 9 Jan 2026
Revised: 23 Jan 2026
Accepted: 5 Mar 2026
Published: 24 Apr 2026

Academic Editor: Yilun Shang
Copy Editor: Fangling Lan
Production Editor: Fangling Lan



Abstract

This paper investigates the consensus problem of heterogeneous second-order multi-agent systems (MASs) via sampling control. First, the corresponding error system is established based on the model of the MASs. Then, two types of control strategies are designed. In the first strategy, time-driven sampling control is adopted, whereas in the second strategy, event-triggered control is applied. Time-varying control gains are also considered. Furthermore, the Lyapunov functional method and matrix theory are used to deduce consensus criteria for second-order heterogeneous MASs under both sampling control and event-triggered control. In addition, since periodic sampling is included in the control strategies in this study, Zeno behavior is naturally avoided. Finally, two numerical examples are provided to demonstrate the validity of the designed control mechanisms.

Check for updates

[1]School of Information and Intelligent Science, Donghua University, Shanghai 201620, China.
[2]School of Science, Nanjing University of Posts and Telecommunications, Nanjing 210023, Jiangsu, China.
[3]School of Mathematics and Statistics, Xinyang Normal University, Xinyang 464000, Henan, China.
[4]School of Automation, Nanjing University of Posts and Telecommunications, Nanjing 210023, China.

Correspondence to: Prof. Zhengxin Wang, School of Science, Nanjing University of Posts and Telecommunications, Nanjing 210023, Jiangsu, China. E-mail: zwang@njupt.edu.cn

1. INTRODUCTION

Over the past few decades, with the widespread application of dynamical systems, increasing attention has been devoted to investigating their dynamic behaviors. Several theoretical results have been reported, including consensus tracking control for multi-agent systems (MASs) with linear nodal dynamics[1], robust non-fragile H_∞ filtering for fuzzy fractional order systems[2], Hopf bifurcation in multiple-delayed predator-prey systems[3], and clustering of genetic regulatory networks[4]. Among these studies, consensus control has attracted significant interest[5,6] and is the central focus of this work.

MASs represent a prevalent class of dynamical systems with broad applications in robot cooperation[7], sensor networks[8], military applications[9], and other fields. Every agent in a MAS can be modeled as a node in a network, and consensus can be achieved with efficiently and flexibly through the exchange of local state information. In early studies on consensus in MASs, most researchers focused on position information as an influencing factor[10,11,12]. In subsequent research, to more accurately characterize agent dynamics, velocity information was incorporated alongside position information. This led to the development of second-order MASs[13,14,15]. Lu *et al.*[13] studied predefined-time consensus of second-order MASs subject to external disturbances using a predefined-time observer. Zhao *et al.*[14] proposed an event-triggered control strategy to investigate consensus in second-order discrete-time MASs influenced by the eigenvalues of the Laplacian matrix. Meng *et al.*[15] examined consensus in a double-integrator MAS under an undirected connected communication topology. The inclusion of velocity information has promoted the study of MAS models. In most existing studies, MAS dynamics are assumed to be homogeneous. However, such an assumption is often idealized, as agents in practical systems rarely exhibit identical dynamics. Compared with homogeneous systems, heterogeneous systems are more general and have higher theoretical significance. For heterogeneous MASs, simple linear feedback controllers cannot achieve complete consensus due to the inherent differences among agent dynamics. Achieving complete consensus would therefore require complex and costly control strategies. Accordingly, this paper focuses on quasi-consensus for second-order heterogeneous MASs, where the consensus errors are guaranteed to converge to a bounded range.

External controllers are essential for accelerating and facilitating consensus in heterogeneous systems. Common approaches include adaptive control[16], intermittent control[17], sampling control[18,19], impulsive control[20], and pinning control[21,22], which are used to address consensus problems in heterogeneous MASs. Specifically, adaptive control provides a strategy for handling time-varying parameters by continuously adjusting them through an adaptive law, thereby effectively regulating the system. In[16], optimal adaptive consensus tracking control for nonlinear MASs with prescribed performance is discussed, where the parameters in the adaptive protocol are adjusted based on the received output information. In practical digital computer systems, continuous signals cannot be directly utilized; instead, signal data must undergo processes such as discretization, sampling, compression, and decompression before they can be processed. Sampling control methods are widely used due to their ease of design and effective implementation in computer-controlled digital systems. For MAS, selecting an appropriate sampling control scheme is not only practical for data communication and controller execution, but also effective in significantly reducing system resource consumption. In[18], consensus of MASs is investigated using dynamic output feedback based on sampled data. Unlike impulsive control, which affects nodes only at discrete instants, sampling control can exert influence over continuous intervals based on sampled information. In[20], a consensus control strategy is proposed for a novel heuristic nonlinear MAS. Compared with previous studies, this research explores a control protocol that integrates both saturation effects and an impulsive control mechanism, demonstrating high efficiency, low cost, and broad applicability. In practice, to reduce control costs, it is common to control only a subset of agents rather than the entire system; this approach is referred to as pinning control. Hao *et al.*[21] investigated group consensus of MASs subject to external disturbances by constructing two pinning control algorithms. In[22], to address consensus in second-order nonlinear MASs under attacks, actuator failures, and integral quadratic constraints, an event-triggered pinning scheme

based on local information was designed. To further reduce costs, sampling control is often combined with pinning control, thereby reducing both control effort and the number of controlled nodes.

In addition to the above control methods, there is another type of controller, namely event-triggered control, which has received significant attention in recent years. Such a controller determines the triggering instants based on predefined event conditions and can achieve consensus while reducing resource consumption and cost by effectively decreasing the number of sampling instances. For example, Yang *et al.*[23] adopted event-triggered control in their research on nonlinear MASs under limited communication resources. Li *et al.*[24] also presented an event-triggered control strategy for time-varying MASs to address parameter uncertainties within a given finite horizon and deception attacks. More recently, to better reflect practical scenarios, dynamic event-triggered control strategies have been proposed[25,26]. Furthermore, studies[22] and[27] have combined pinning control and sampling control with event-triggered control to reach consensus in MASs. In[22], the authors mainly focus on cluster consensus in the presence of acyclic denial-of-service (DoS) attacks, actuator failures, and integral quadratic constraints. In[27], the synchronization problem of first-order MASs with time-varying control gains is investigated under a synchronous periodic sampling framework. However, it does not consider factors such as network attacks or actuator faults; instead, it mainly addresses the synchronization control of nonlinear agents based on sampled data in directed topologies. In addition, in[28], the authors propose both an observer-based event-triggered controller and an observer-based full asynchronous event-triggered controller to study the bipartite consensus problem of MASs under unknown false data injection attack. Event-triggered control has been widely applied in the field of control systems. It can be used not only in consensus studies of MASs but also in investigating annular finite-time H_∞ performance in complex networks[29].

In this work, by leveraging the advantages of event-triggered control, sampling control, and pinning control, two novel hybrid controllers are designed to achieve consensus in heterogeneous second-order nonlinear MASs. The effectiveness of the proposed methods is demonstrated through numerical examples. Furthermore, the main contributions of this paper are summarized below.

(i) At present, there is limited literature on consensus in heterogeneous second-order MASs. In this paper, by studying such systems, sufficient criteria for achieving consensus are established.

(ii) Although hybrid controllers have made great progress in the past decade, there remains room for improvement in their application to heterogeneous second-order MASs. By integrating event-triggered control, sampling control, and pinning control, the control duration, the number of sampling instances, and the number of controlled nodes are reduced, thereby saving resources.

(iii) The sampling control adopted in this paper effectively avoids Zeno behavior. It is important to note that since triggering instants occur only at sampling instants, the lower bound of the inter-event times is equal to the sampling period.

2. PRELIMINARIES

In this section, the notation and models for a heterogeneous second-order MAS comprising one leader and N followers are presented.

2.1. Notations

The symbols $\mathbb{R}$ and $\mathbb{Z}_+$ denote the sets of real numbers and positive integers, respectively. Furthermore, $\mathbb{R}^n$ and $\mathbb{R}^{n\times m}$ indicate the sets of n-dimensional real vectors and $n\times m$ real matrices, respectively. For a symmetric matrix A, $\lambda_{\max}(A)$ and $\lambda_{\min}(A)$ denote its maximum and minimum eigenvalues, respectively. $A > 0$ means that A is positive

definite. Let $A = (a_{ij})_{N\times N}$ be the weighted adjacency matrix of an undirected graph $\mathcal{G}$, and the corresponding Laplacian matrix is defined as $L = (l_{ij})_{N\times N}$, where $l_{ij} = a_{ij}$ for $i \neq j$ and $l_{ij} = \sum_{i\neq j} a_{ij}$ for $i = j$. The symbol E is the identity matrix.

2.2 Model description

Consider a second-order heterogeneous nonlinear MAS composed of one leader and N followers. The first N agents are followers, and the $(N+1)$th agent is the leader, which is an isolated node and is not influenced by other nodes. The dynamics of the leader is given by

$$\ddot{x}_{N+1}(t) = h_{N+1}(t, x_{N+1}(t), \dot{x}_{N+1}(t)). \tag{1}$$

The dynamics of the N followers are modeled by

$$\ddot{x}_i(t) = h_i(t, x_i(t), \dot{x}_i(t)) + u_i(t), i \in \mathcal{N} = \{1, 2, \cdots, N\}. \tag{2}$$

Let $\dot{x}_{N+1}(t) = v_{N+1}(t)$ and $\dot{x}_i(t) = v_i(t)$. Then system (1) can be rewritten as

$$\begin{cases} \dot{x}_{N+1}(t) = \dot{v}_{N+1}(t), \\ \dot{v}_{N+1}(t) = h_{N+1}(t, x_{N+1}(t), v_{N+1}(t)), \end{cases} \tag{3}$$

and

$$\begin{cases} \dot{x}_i(t) = \dot{v}_i(t), \\ \dot{v}_i(t) = h_i(t, x_i(t), v_i(t)) + u_i(t), \end{cases} \tag{4}$$

where $x_i(t), v_i(t)$, and $h_i(t, x_i(t), v_i(t)) \in \mathbb{R}^n$ represent the position state, velocity state, and intrinsic dynamics of the ith node. Moreover, $h_i(t, x_i(t), v_i(t))$ is assumed to be continuous, and $u_i(t)$ is the external control input to be proposed.

3. MAIN RESULTS

This section designs pinning sampling controllers to achieve consensus in heterogeneous second-order nonlinear MASs (1) and (2). The investigation is divided into two subsections: consensus under sampling control and consensus under hybrid event-triggered sampling control. Furthermore, a detailed derivation of the consensus process for the MASs is given below.

3.1 Leader-follower consensus under sampling control

Define the consensus errors as $\hat{x}_i(t) = x_i(t) - x_{N+1}(t)$ and $\hat{v}_i(t) = v_i(t) - v_{N+1}(t)$, for $i \in \mathcal{N}$. Then, the error dynamics are given by

$$\begin{cases} \dot{\hat{x}}_i(t) = \hat{v}_i(t), \\ \dot{\hat{v}}_i(t) = h_i(t, x_i(t), v_i(t)) - h_{N+1}(t, x_{N+1}(t), v_{N+1}(t)) - u_i(t), \end{cases} \tag{5}$$

for $i \in \mathcal{N}$. The sampling period is h, and the agent states are available at sampling instants $\mathcal{T} = \{T_l\}_{l\in\mathbb{Z}_+}$, where $T_l = T_0 + lh$ with $T_0 = 0$. Then, the sampling control law $u_i^1(t)$ is designed as

$$\begin{aligned} u_i^1(t) =& \alpha(t)[\Sigma_{j=1}^N a_{ij}(x_j(lh) - x_i(lh)) - \varrho_i(x_i(lh) - x_{N+1}(lh))] \\ &+ \beta(t)[\Sigma_{j=1}^N a_{ij}(v_j(lh) - v_i(lh)) - \varrho_i(v_i(lh) - v_{N+1}(lh))], \end{aligned} \tag{6}$$

where $i \in \mathcal{N}$. The functions $\alpha(t) \geq 0$ and $\beta(t) \geq 0$ denote bounded control gains, and $\varrho_i > 0$ represents the pinning control gain. The flowchart for sampling control $u_i^1(t)$ is shown in Figure 1.

Given that $x(t) = (x_1^T(t), x_2^T(t), \cdots, x_N^T(t))^T$, $v(t) = (v_1^T(t), v_2^T(t), \cdots, v_N^T(t))^T$, $\hat{x}(t) = (\hat{x}_1^T(t), \hat{x}_2^T(t), \cdots, \hat{x}_N^T(t))^T$, $\hat{v}(t) = (\hat{v}_1^T(t), \hat{v}_2^T(t), \cdots, \hat{v}_N^T(t))^T$, $H(t, x(t), v(t)) = (h_1^T(t, x_1, v_1), h_2^T(t, x_2, v_2), \cdots, h_N^T(t, x_N, v_N))^T$, $\hat{H}(t, x_{N+1}(t), v_{N+1}(t)) = ((h_1 - h_{N+1})^T(t, x_{N+1}, v_{N+1}), (h_2 - h_{N+1})^T(t, x_{N+1}, v_{N+1}), \cdots, (h_N - h_{N+1})^T(t, x_{N+1}, v_{N+1}))^T$, $\Upsilon = diag\{\varrho_1, \varrho_2, \cdots, \varrho_N\}$, system (5) can be rewritten as

$$\begin{cases} \dot{\hat{x}}(t) = \hat{v}(t), \\ \dot{\hat{v}}(t) = H(t, x(t), v(t)) - H(t, X_{N+1}(t), V_{N+1}(t)) + \hat{H}(t, X_{N+1}(t), V_{N+1}(t)) \\ \qquad - \alpha(t)((L + \Upsilon) \otimes I_n) \cdot \hat{x}(lh) - \beta(t)((L + \Upsilon) \otimes I_n) \cdot \hat{v}(lh), \end{cases} \tag{7}$$

where $X_{N+1} = 1_N \otimes x_{N+1}$, $V_{N+1} = 1_N \otimes v_{N+1}$.

Assumption 1. *The function H in (7) satisfies the global Lipschitz condition, that is,*

$$\|H(t, x, v) - H(t, y, z)\| \leq \rho_1 \|x - y\| + \rho_2 \|v - z\|, \forall x, y, v, z \in \mathbb{R}^n,$$

where $\rho_1 \geq 0$ and $\rho_2 \geq 0$.

Assumption 2. *The leader state is bounded, which implies that the function $\hat{H}$ in (7) is also bounded under any initial condition. Specifically, there is a constant $\chi > 0$ such that $\sup_{-h \leq s \leq 0} \|\hat{H}(t + s, x_{N+1}(t + s), v_{N+1}(t + s))\| = \chi$.*

Remark 1. *The global Lipschitz condition in Assumption 1 is a standard assumption for deriving explicit stability criteria. In practice, for locally Lipschitz nonlinear systems, this condition can be interpreted as requiring a sufficiently large Lipschitz constant valid over the bounded operational region ensured by the closed-loop system. For systems exhibiting unbounded nonlinear growth, techniques such as input saturation may be introduced to guarantee boundedness.*

Remark 2. *The leader's state may correspond to a stable equilibrium, periodic orbit, or chaotic attractor. Therefore, it is reasonable to assume that the leader state is bounded. Since $\hat{H}$ is a continuous function of the leader state, it is also bounded.*

Remark 3. *As for pinning control, the selection of pinned nodes is crucial. If the communication topology is disconnected, at least one node in each connected component should be pinned. Otherwise, any node can be selected as a pinned node. The pinning strength ϱ_i can then be assigned accordingly.*

Theorem 1. *Under Assumptions 1-2 and controller (6), the MASs (1) and (2) can achieve quasi-consensus exponentially if there exist a constant $\theta > 0$ and a positive definite matrix $J > 0$ satisfying*

$$\zeta_1(t) + \zeta_2(t) \leq -\theta < 0, \tag{8}$$

and

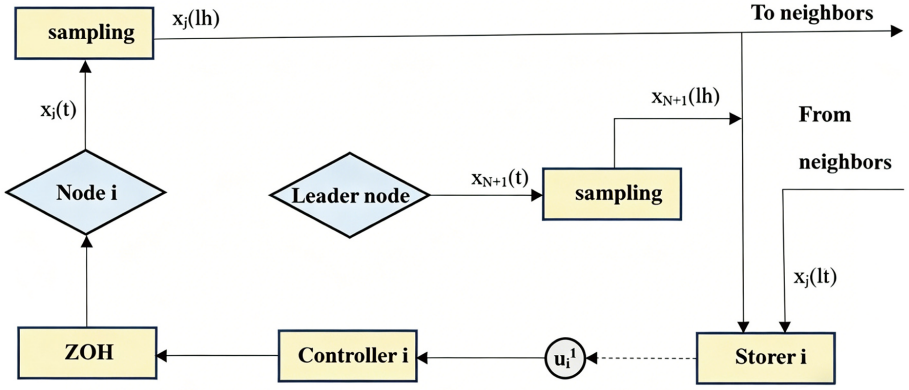


Figure 1. Flowchart of sampling control $u_i^1(t)$.

$$C - J > 0, \tag{9}$$

where $\zeta_1(t) = \frac{1}{\|\Xi\|}\max\{1+\|J\|\cdot(3\rho_1+\rho_2+1)+(\alpha(t)+\beta(t)\rho_1^2)h\cdot\|J(L+\Upsilon)\|+2\beta(t)h\cdot(1+\rho_1)\cdot\|J(L+\Upsilon)\|+(\alpha(t)+\beta(t))\beta(t)h\cdot\|J(L+\Upsilon)\|\cdot\|L+\Upsilon\|-\alpha(t)\cdot\lambda_{\min}[J(L+\Upsilon)+(L+\Upsilon)J], \|J\|\cdot(3\rho_2+\rho_1+1)+(\alpha(t)+\beta(t)\rho_2)h\cdot\|J(L+\Upsilon)\|+2\beta(t)h\cdot(1+\rho_2)\cdot\|J(L+\Upsilon)\|+(\alpha(t)+\beta(t))\beta(t)h\cdot\|J(L+\Upsilon)\|\cdot\|L+\Upsilon\|+2\lambda_{\max}(J)-\beta(t)\cdot\lambda_{\min}[J(L+\Upsilon)+(L+\Upsilon)J]\} \le 0$, $\zeta_2(t) = \frac{1}{\|\Xi\|}\max\{2\alpha(t)\beta(t)h\cdot\|J(L+\Upsilon)\|\cdot\|L+\Upsilon\|, (\alpha(t)+2\beta(t)^2\cdot\|L+\Upsilon\|)\cdot\|J(L+\Upsilon)\|\cdot h\} \ge 0$, $C = \min\{\underline{\beta}, \underline{\alpha}\}\cdot[J(L+\Upsilon)+(L+\Upsilon)J]$, $\underline{\alpha} = \min\{\alpha(t)\} > 0$, *and* $\underline{\beta} = \min\{\beta(t)\} > 0$.

Proof. *For* $t \in [lh, (l+1)h)$, *define* $V_1(t) = \hat{z}^T(t)(\Xi \otimes I_n)\hat{z}(t)$ *with* $\hat{z}(t) = (\hat{x}^T(t), \hat{v}^T(t))^T$ *and* $\Xi = \begin{pmatrix} C & J \\ J & J \end{pmatrix}$. *We calculate* $\dot{v}_1(t)$ *and substitute the trajectories of (7) into* $\dot{v}_1(t)$,

$$\begin{aligned}
\dot{V}_1(t) =& 2\hat{x}^T(t)(C\otimes I_n)\dot{\hat{x}}(t) + 2\hat{x}^T(t)(J\otimes I_n)\dot{\hat{v}}(t) + 2\hat{v}^T(t)(J\otimes I_n)\dot{\hat{x}}(t) + 2\hat{v}^T(t)(J\otimes I_n)\dot{\hat{v}}(t)\\
=& 2\hat{x}^T(t)(C\otimes I_n)\hat{v}(t) + 2\hat{v}^T(t)(J\otimes I_n)\hat{v}(t) + 2\hat{x}^T(t)(J\otimes I_n)[H(t,x(t),v(t))\\
&+ \hat{H}(t,x_{N+1}(t),v_{N+1}(t)) - \alpha(t)((L+\Upsilon)\otimes I_n)\hat{x}(lh) - \beta(t)((L+\Upsilon)\otimes I_n)\hat{v}(lh)]\\
&+ 2\hat{v}^T(t)(J\otimes I_n) - H(t,X_{N+1}(t),V_{N+1}(t))(H(t,x(t),v(t)) - H(t,X_{N+1}(t),V_{N+1}(t))\\
&+ \hat{H}(t,x_{N+1}(t),v_{N+1}(t)) - \alpha(t)((L+\Upsilon)\otimes I_n)\hat{x}(lh) - \beta(t)((L+\Upsilon)\otimes I_n)\hat{v}(lh)).
\end{aligned} \tag{10}$$

Then, we obtain

$$\begin{aligned}
&2\hat{x}^T(t)(J\otimes I_n)(H(t,x(t),v(t)) - H(t,X_{N+1}(t),V_{N+1}(t)))\\
\le& 2\|\hat{x}(t)\|\cdot\|J\|\cdot\|H(t,x(t),v(t)) - H(t,X_{N+1}(t),V_{N+1}(t))\|\\
\le& \|J\|\cdot[(2\rho_1+\rho_2)\cdot\|\hat{x}(t)\|^2 + \rho_2\cdot\|\hat{v}(t)\|^2],
\end{aligned} \tag{11}$$

and

$$2\hat{x}^T(t)(J\otimes I_n)\hat{H}(t,x_{N+1}(t),v_{N+1}(t)) \le \|J\|\cdot(\|\hat{x}(t)\|^2 + \chi^2). \tag{12}$$

Furthermore, we have

$$\begin{aligned}
&2\hat{x}^T(t)(J\otimes I_n)[-\alpha(t)((L+\Upsilon)\otimes I_n)\hat{x}(lh)]\\
=&2\alpha(t)\hat{x}^T(t)(J(L+\Upsilon)\otimes I_n)\int_{t-\tau(t)}^{t}\dot{\hat{x}}(s)ds-2\alpha(t)\hat{x}^T(t)(J(L+\Upsilon)\otimes I_n)\hat{x}(t)\\
\le&\alpha(t)h\cdot\|J(L+\Upsilon)\|\cdot(\|\hat{x}(t)\|^2+(\sup_{-h\le s\le 0}\|\hat{v}(t+s)\|)^2)-\alpha(t)\cdot\lambda_{\min}[J(L+\Upsilon)\\
&+(L+\Upsilon)J]\cdot\|\hat{x}(t)\|^2,
\end{aligned}\tag{13}$$

and

$$\begin{aligned}
&2\hat{x}^T(t)(J\otimes I_n)[-\beta(t)((L+\Upsilon)\otimes I_n)\hat{v}(lh)]\\
=&2\beta(t)\hat{x}^T(t)(J(L+\Upsilon)\otimes I_n)\int_{t-\tau(t)}^{t}\dot{\hat{v}}(s)ds-2\beta(t)\hat{x}^T(t)(J(L+\Upsilon)\otimes I_n)\hat{v}(t)\\
\le&2\beta(t)h\rho_1\cdot\|J(L+\Upsilon)\|\cdot\|\hat{x}(t)\|^2+\beta(t)h\cdot\|J(L+\Upsilon)\|\cdot(2\|\hat{x}(t)\|^2+\rho_2^2\cdot\|\hat{v}(t)\|^2+\chi^2)\\
&+\beta(t)\alpha(t)h\cdot\|J(L+\Upsilon)\|\cdot\|L+\Upsilon\|\cdot(\|\hat{x}(t)\|^2+(\sup_{-h\le s\le 0}\|\hat{x}(t+s)\|))^2+\beta^2(t)h\\
&\|J(L+\Upsilon)\|\cdot\|L+\Upsilon\|(\|\hat{x}(t)\|^2+(\sup_{-h\le s\le 0}\|\hat{v}(t+s)\|)^2)-2\beta(t)\hat{x}^T(t)(J(L+\Upsilon)\otimes I_n)\hat{v}(t).
\end{aligned}\tag{14}$$

Similarly, we obtain the following deduction,

$$\begin{aligned}
&2\hat{v}^T(t)(J\otimes I_n)(H(t,x(t),v(t))-H(t,X_{N+1}(t),V_{N+1}(t)))\\
\le&\|J\|\cdot[(2\rho_2+\rho_1)\cdot\|\hat{v}(t)\|^2+\rho_1\cdot\|\hat{x}(t)\|^2],
\end{aligned}\tag{15}$$

$$2\hat{v}^T(t)(J\otimes I_n)\hat{H}(t,x_{N+1}(t),v_{N+1}(t))\le\quad\|J\|\cdot(\|\hat{v}(t)\|^2+\chi^2),\tag{16}$$

$$\begin{aligned}
&2\hat{v}^T(t)(J\otimes I_n)[-\alpha(t)((L+\Upsilon)\otimes I_n)\hat{x}(lh)]\\
\le&\alpha(t)h\cdot\|J(L+\Upsilon)\|\cdot(\|\hat{v}(t)\|^2+(\sup_{-h\le s\le 0}\|\hat{v}(t+s)\|)^2)-2\alpha(t)\hat{v}^T(t)(J(L+\Upsilon)\otimes I_n)\hat{x}(t),
\end{aligned}\tag{17}$$

and

$$\begin{aligned}
&2\hat{v}^T(t)(J\otimes I_n)[-\beta(t)((L+\Upsilon)\otimes I_n)\hat{v}(lh)]\\
\le&2\beta(t)h\rho_2\cdot\|J(L+\Upsilon)\|\cdot\|\hat{v}(t)\|^2+\beta(t)h\cdot\|J(L+\Upsilon)\|\cdot(2\|\hat{v}(t)\|^2+\rho_1^2\cdot\|\hat{v}(t)\|^2+\chi^2)\\
&+\beta(t)\alpha(t)h\cdot\|J(L+\Upsilon)\|\cdot\|L+\Upsilon\|\cdot(\|\hat{v}(t)\|^2+(\sup_{-h\le s\le 0}\|\hat{x}(t+s)\|))^2+\beta^2(t)h\\
&\|J(L+\Upsilon)\|\cdot\|L+\Upsilon\|(\|\hat{v}(t)\|^2+(\sup_{-h\le s\le 0}\|\hat{v}(t+s)\|))^2-\beta(t)\lambda_{\min}[J(L+\Upsilon)\\
&+(L+\Upsilon)J]\|\hat{v}(t)\|^2.
\end{aligned}\tag{18}$$

Applying (11)-(18) yields

$$\dot{V}_1(t)\le\zeta_1(t)V_1(t)+\zeta_2(t)\sup_{-h\le s\le 0}V_1(t+s)+\zeta_3,\tag{19}$$

where $\zeta_3=\frac{(2\|J\|+10h\cdot\|J(L+\Upsilon)\|)\chi^2}{\|\Xi\|}$.

By Theorem 2.3 in[30]*, we obtain* $V_1(t) \le \frac{\zeta_3}{\theta} + V_1(0)$. *Consequently,*

$$\|\hat{z}(t)\|^2 \le \frac{V_1(t)}{\lambda_{\min}(\Xi)} \le \frac{\frac{\zeta_3}{\theta} + V_1(0)}{\lambda_{\min}(\Xi)}, \tag{20}$$

Therefore, the heterogeneous second-order MASs (1) and (2) can realize quasi-consensus.

Remark 4. *Notably, the matrix blocks* C *and* J *in matrix* Υ *are* $N \times N$ *square matrices. By the Schur complement lemma*[31]*, it follows that* $\Xi > 0$ *is equivalent to* $C > J > 0$. *Therefore, to ensure* $\Xi > 0$, *the condition* $\Delta = \min\{\underline{\beta}, \underline{\alpha}\} \cdot [J(L + \Upsilon) + (L + \Upsilon)J] - J > 0$ *should hold.*

Remark 5. *The coupling strengths* $\alpha(t)$ *and* $\beta(t)$ *used in this paper are time-varying, meaning that they can change over time. Compared to constant coupling strengths, time-varying coupling strengths are more suitable for describing dynamic interactions among agents. In practice, the coupling strength between agents is often influenced by factors such as relative distance and energy, both of which vary over time.*

3.2 Lead-following consensus under event-triggered control

In this subsection, a hybrid control strategy that combines the controller in (6) with an event-triggered mechanism is represented as follows

$$\begin{aligned} u_i^2(t) =& \alpha(t)[\Sigma_{j=1}^N a_{ij}(\tilde{x}_j(t) - \tilde{x}_i(t)) - \varrho_i(\tilde{x}_i(t) - x_{N+1}(lh))] \\ &+ \beta(t)[\Sigma_{j=1}^N a_{ij}(\tilde{v}_j(t) - \tilde{v}_i(t)) - \varrho_i(\tilde{v}_i(t) - v_{N+1}(lh))], \end{aligned} \tag{21}$$

where $i \in \mathcal{N}$ and $t \in [lh, (l+1)h)$. The sampled states are defined as $\tilde{x}_i(t) = x_i(t^i_{k_i} h)$ and $\tilde{v}_i(t) = v_i(t^i_{k_i} h)$ for $t \in [t^i_{k_i} h, t^i_{k_i+1} h)$. The functions $\alpha(t) \ge 0$ and $\beta(t) \ge 0$ represent bounded time-varying control gains , and ϱ_i is a positive constant representing the pinning control gain. The sequence $\{t_{k_i} h\}_{k_i \in \mathbb{Z}_+} \subseteq \mathcal{T}$ represents the event-triggered instants, which occur only at selected sampling moments. The flowchart of the event-triggered control $u_i^2(t)$ is shown in Figure 2.

Define $\delta_i^x(t) = x_i(t) - x_i(t^i_{k_i} h)$ and $\delta_i^v(t) = v_i(t) - v_i(t^i_{k_i} h)$ as the measurement errors for $t \in [t^i_{k_i} h, t^i_{k_i+1} h)$. Let $\delta^x(t) = (\delta_1^{xT}(t), \delta_2^{xT}(t), \cdots, \delta_N^{xT}(t))^T$ and $\delta^v(t) = (\delta_1^{vT}(t), \delta_2^{vT}(t), \cdots, \delta_N^{vT}(t))^T$. Then, we get

$$\begin{cases} \dot{\hat{x}}(t) = \hat{v}(t), \\ \dot{\hat{v}}(t) = H(t, x(t), v(t)) - H(t, X_{N+1}(t), V_{N+1}(t)) + \hat{H}(t, X_{N+1}(t), V_{N+1}(t)) \\ \qquad - \alpha(t)((L + \Upsilon) \otimes I_n) \cdot \hat{x}(lh) - \beta(t)((L + \Upsilon) \otimes I_n) \cdot \hat{v}(lh) \\ \qquad + \alpha(t)((L + \Upsilon) \otimes I_n) \cdot \delta^x(lh) + \beta(t)((L + \Upsilon) \otimes I_n) \cdot \delta^v(lh), \end{cases} \tag{22}$$

where $t \in [lh, (l+1)h)$, $X_{N+1} = 1_N \otimes x_{N+1}$, and $V_{N+1} = 1_N \otimes v_{N+1}$.

Furthermore, the triggering instant $t^i_{k_i} h$ is determined as follows

$$\begin{aligned} t^i_{k_{i+1}} h =& t^i_{k_i} h + \inf\Big\{mh \big| \bar{\alpha}^2 \|\delta_i^x(t^i_{k_i} h + mh)\|^2 + \bar{\beta}^2 \|\delta_i^v(t^i_{k_i} h + mh)\|^2 \ge \sigma_i(\|\hat{x}_i(t^i_{k_i} h + mh)\|^2 \\ &+ \|\hat{v}_i(t^i_{k_i} h + mh)\|^2)\Big\}, \end{aligned} \tag{23}$$

where $\bar{\alpha} = \max\{\alpha(t)\} > 0$, $\bar{\beta} = \max\{\beta(t)\} > 0$, and $\bar{\sigma} = \max\{\sigma_i\}$. Notably, the triggering instants occur only at discrete sampling instants. Therefore, the minimum interval between two consecutive triggering instants is the sampling period h, which naturally excludes Zeno behavior.

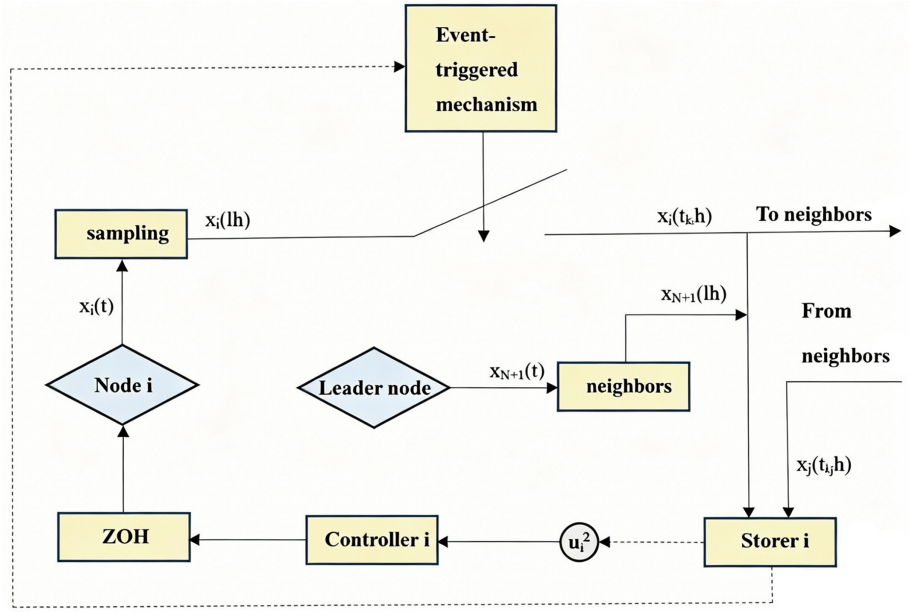


Figure 2. Flowchart of the event-triggered control $u_i^2(t)$.

Theorem 2. *Base on Assumptions 1-2 and controller (21), the MASs (1) and (2) can realize quasi-consensus exponentially if there is a constant $\theta > 0$ and a matrix $J > 0$ satisfying*

$$\tilde{\zeta}_1(t) + \zeta_2(t) \le -\theta < 0, \tag{24}$$

and

$$C - J > 0, \tag{25}$$

where $\tilde{\zeta}_1(t) = \frac{1}{\|\Xi\|}\max\{1+\|J\|\cdot(3\rho_1+\rho_2+1)+(\alpha(t)+\beta(t)\rho_1^2)h\cdot\|J(L+\Upsilon)\|+2\beta(t)h\cdot(1+\rho_1)\cdot\|J(L+\Upsilon)\|+4\|JL\|+(\alpha(t)+\beta(t))\beta(t)h\cdot\|J(L+\Upsilon)\|\cdot\|L+\Upsilon\|+2\bar{\sigma}\beta(t)h\cdot\|J(L+\Upsilon)\|\cdot\|L\|-\alpha(t)\cdot\lambda_{\min}[J(L+\Upsilon)+(L+\Upsilon)J, \|J\|\cdot(3\rho_2+\rho_1+1)+(\alpha(t)+\beta(t)\rho_2)h\cdot\|J(L+\Upsilon)\|+2\beta(t)h\cdot(1+\rho_2)\cdot\|J(L+\Upsilon)\|+4\|JL\|+(\alpha(t)+\beta(t))\beta(t)h\cdot\|J(L+\Upsilon)\|\cdot\|L+\Upsilon\|+2\lambda_{\max}(J)+2\bar{\sigma}\beta(t)h\cdot\|J(L+\Upsilon)\|\cdot\|L\|-\beta(t)\cdot\lambda_{\min}[J(L+\Upsilon)+(L+\Upsilon)J]\} \le 0$ *and* $\zeta_2(t) = \frac{1}{\|\Xi\|}\max\{2\alpha(t)\beta(t)h\cdot\|J(L+\Upsilon)\|\cdot\|L+\Upsilon\|, (\alpha(t)+2\beta^2(t)\cdot\|L+\Upsilon\|)\cdot\|J(L+\Upsilon)\|\cdot h\} \ge 0$, $C = \min\{\underline{\beta}, \underline{\alpha}\}\cdot[J(L+\Upsilon)+(L+\Upsilon)J]$, $\underline{\alpha} = \min\{\alpha(t)\} > 0$, *and* $\underline{\beta} = \min\{\beta(t)\} > 0$.

Proof. *For* $t \in [lh, (l+1)h)$, *define* $V_2(t) = \hat{z}^T(t)(\Xi \otimes I_n)\hat{z}(t)$ *with* $\Xi = \begin{pmatrix} C & J \\ J & J \end{pmatrix}$ *and* $\hat{z}(t) = (\hat{x}^T(t), \hat{v}^T(t))^T$. *Then*

$$\begin{aligned} V_2(t) &= \begin{pmatrix} \hat{x}^T(t) & \hat{v}^T(t) \end{pmatrix}\left[\begin{pmatrix} C & J \\ J & J \end{pmatrix}\otimes I_n\right]\begin{pmatrix} \hat{x}(t) \\ \hat{v}(t) \end{pmatrix} \\ &= \hat{x}^T(t)(C\otimes I_n)\hat{x}(t) + 2\hat{x}^T(t)(J\otimes I_n)\hat{v}(t) + \hat{v}^T(t)(J\otimes I_n)\hat{v}(t). \end{aligned} \tag{26}$$

Taking the derivative of $V_2(t)$ *and substituting the trajectories from (22) into* $V_2(t)$, *we obtain*

$$\begin{aligned}\dot{V}_2(t) =&2\hat{x}^T(t)(C\otimes I_n)\dot{\hat{x}}(t)+2\hat{x}^T(t)(J\otimes I_n)\dot{\hat{v}}(t)+2\hat{v}^T(t)(J\otimes I_n)\dot{\hat{x}}(t)+2\hat{v}^T(t)(J\otimes I_n)\dot{\hat{v}}(t)\\ =&2\hat{x}^T(t)(C\otimes I_n)\hat{v}(t)+2\hat{v}^T(t)(J\otimes I_n)\hat{v}(t)+2\hat{x}^T(t)(J\otimes I_n)[H(t,x(t),v(t))\\ &-H(t,X_{N+1}(t),V_{N+1}(t))+\hat{H}(t,x_{N+1}(t),v_{N+1}(t))-\alpha(t)((L+\Upsilon)\otimes I_n)\hat{x}(lh)\\ &-\beta(t)((L+\Upsilon)\otimes I_n)\hat{v}(lh)+\alpha(t)((L+\Upsilon)\otimes I_n)\delta^x(lh)+\beta(t)((L+\Upsilon)\otimes I_n)\cdot\delta^v(lh)]\\ &+2\hat{v}^T(t)(J\otimes I_n)[H(t,x(t),v(t))-H(t,X_{N+1}(t),V_{N+1}(t))+\hat{H}(t,x_{N+1}(t),v_{N+1}(t))\\ &-\alpha(t)((L+\Upsilon)\otimes I_n)\hat{x}(lh)-\beta(t)((L+\Upsilon)\otimes I_n)\hat{v}(lh)+\alpha(t)((L+\Upsilon)\otimes I_n)\\ &\delta^x(lh)+\beta(t)((L+\Upsilon)\otimes I_n)\cdot\delta^v(lh)].\end{aligned}\tag{27}$$

Then, we have

$$\begin{aligned}&2\hat{x}^T(t)(J\otimes I_n)[\alpha(t)((L+\Upsilon)\otimes I_n)\delta^x(lh)+\beta(t)(L\otimes I_n)\delta^v(lh)]\\ &+2\hat{v}^T(t)(J\otimes I_n)[\alpha(t)((L+\Upsilon)\otimes I_n)\delta^x(lh)+\beta(t)(L\otimes I_n)\delta^v(lh)]\\ \le&2\cdot\|J(L+\Upsilon)\|\cdot\|\hat{x}(t)+\hat{v}(t)\|\cdot\|\alpha(t)\delta^x(lh)+\beta(t)\delta^v(lh)\|\\ \le&2\|J(L+\Upsilon)\|(\|\hat{x}(t)\|^2+\|\hat{v}(t)\|^2+\bar{\alpha}^2\cdot\|\delta^x(lh)\|^2+\bar{\beta}^2\cdot\|\delta^v(lh)\|^2).\end{aligned}\tag{28}$$

In addition, we have

$$\begin{aligned}&2\hat{x}^T(t)(J\otimes I_n)[-\beta(t)((L+\Upsilon)\otimes I_n)\hat{v}(lh)]\\ =&2\beta(t)\hat{x}^T(t)(J(L+\Upsilon)\otimes I_n)\int_{t-\tau(t)}^{t}\dot{\hat{v}}(s)ds-2\beta\hat{x}^T(t)(J(L+\Upsilon)\otimes I_n)\hat{v}(t)\\ \le&2\beta(t)h\rho_1\cdot\|J(L+\Upsilon)\|\cdot\|\hat{x}(t)\|^2+\beta(t)h\cdot\|J(L+\Upsilon)\|\cdot[2(1+\|L\|)\cdot\|\hat{x}(t)\|^2\\ &+\rho_2^2\cdot\|\hat{v}(t)\|^2+\chi^2]+\beta(t)\alpha(t)h\cdot\|J(L+\Upsilon)\|\cdot\|L+\Upsilon\|\cdot(\|\hat{x}(t)\|^2+(\sup_{-h\le s\le 0}\|\hat{x}(t+s)\|)^2)\\ &+\beta^2(t)h\cdot\|J(L+\Upsilon)\|\cdot\|L+\Upsilon\|(\|\hat{x}(t)\|^2+(\sup_{-h\le s\le 0}\|\hat{v}(t+s)\|)^2)-2\beta(t)\hat{x}^T(t)\\ &(J(L+\Upsilon)\otimes I_n)\hat{v}(t)+\beta(t)h\cdot\|J(L+\Upsilon)\|\cdot\|L+\Upsilon\|(\bar{\alpha}^2\cdot\|\delta^x(lh)\|^2+\bar{\beta}^2\cdot\|\delta^v(lh)\|^2),\end{aligned}\tag{29}$$

and

$$\begin{aligned}&2\hat{v}^T(t)(J\otimes I_n)[-\beta(t)((L+\Upsilon)\otimes I_n)\hat{v}(lh)]\\ =&2\beta(t)\hat{v}^T(t)(J(L+\Upsilon)\otimes I_n)\int_{t-\tau(t)}^{t}\dot{\hat{v}}(s)ds-2\beta\hat{v}^T(t)(J(L+\Upsilon)\otimes I_n)\hat{v}(t)\\ \le&2\beta(t)h\rho_2\cdot\|J(L+\Upsilon)\|\cdot\|\hat{v}(t)\|^2+\beta(t)h\cdot\|J(L+\Upsilon)\|\cdot[2(1+\|L\|)\cdot\|\hat{v}(t)\|^2\\ &+\rho_1^2\cdot\|\hat{v}(t)\|^2+\chi^2]+\beta(t)\alpha(t)h\cdot\|J(L+\Upsilon)\|\cdot\|L+\Upsilon\|\cdot(\|\hat{v}(t)\|^2\\ &+(\sup_{-h\le s\le 0}\|\hat{x}(t+s)\|))^2+\beta^2(t)h\cdot\|J(L+\Upsilon)\|\cdot\|L+\Upsilon\|(\|\hat{v}(t)\|^2+(\sup_{-h\le s\le 0}\|\hat{v}(t+s)\|))^2\\ &+\beta(t)h\cdot\|J(L+\Upsilon)\|\cdot\|L+\Upsilon\|\cdot(\bar{\alpha}^2\cdot\|\delta^x(lh)\|^2+\bar{\beta}^2\cdot\|\delta^v(lh)\|^2)\\ &-\beta(t)\cdot\lambda_{\min}[J(L+\Upsilon)+(L+\Upsilon)J]\cdot\|\hat{v}(t)\|^2.\end{aligned}\tag{30}$$

Applying (11)-(13), (15)-(17), and (28)-(30), and combining these with the event-triggered strategy (23), we obtain

$$\dot{V}_2(t)\le\tilde{\zeta}_1(t)V_2(t)+\zeta_2(t)\sup_{-h\le s\le 0}V_2(t+s)+\zeta_3,\tag{31}$$

where $\zeta_3(t) = \frac{(2\|J\|+10h\cdot\|J(L+\Upsilon)\|)\chi^2}{\|\Xi\|}$.

The remainder of the proof is similar to that of Theorem 1. Therefore, the heterogeneous second-order MASs (1) and (2) can realize quasi-consensus.

Remark 6. *Since heterogeneous systems are considered in this paper, quasi-consensus is analyzed in both Theorem 1 and Theorem 2. According to (20), the upper bound of the error* $\|\hat{z}(t)\|$ *is related to the constant* χ *and the initial conditions. When the system is homogeneous (i.e.,* $\chi = 0$*), the upper bound of the error becomes smaller and the system achieves improved consensus performance.*

Remark 7. *The threshold parameters* $\sigma_i > 0$ *in (23) play a critical role in balancing consensus performance against communication and computational resource usage. Their selection is guided by the following trade-off consideration. A larger* σ_i *makes the triggering condition more difficult to satisfy, leading to fewer control updates but potentially a larger ultimate bound for the quasi-consensus error. Conversely, a smaller* σ_i *yields more frequent updates and closer tracking performance, approaching that of purely time-driven sampling control, at the cost of increased resource consumption. In this study, the parameters* σ_i *are chosen as fixed values. A principled selection method can be derived from the stability analysis. Specifically, examining the term* $2\bar{\sigma}\beta(t)h\|J(L+\Gamma)\|\|L\|$ *in the coefficient* $\tilde{\zeta}_1(t)$ *in Theorem 2 reveals that* σ_i *directly influences the negativity required for* $\tilde{\zeta}_1(t) + \zeta_2(t) \le -\theta < 0$*. Therefore, to ensure stability,* σ_i *cannot be arbitrarily large and must satisfy constraints imposed by other system parameters. The values used in the simulations (*$\sigma_i = \{10, 20, 10, 20, 10\}$*) are chosen heuristically to satisfy these conditions while demonstrating the effectiveness of the event-triggered mechanism. In practice, these parameters can be tuned offline to achieve a desired trade-off or adapted online within the stability bounds.*

4. SIMULATIONS

This section provides two examples to explain the above results. Specifically, Theorem 1 and Theorem 2 are illustrated in Example 1 and Example 2, respectively. In addition, both connected and disconnected graphs are discussed in the two examples. Consider systems (1) and (2) with $N = 6$ and $n = 2$, where the sixth node is the leader and the remaining five nodes are followers. The initial conditions are given as $x_1(0) = (-5, 2)^T$, $x_2(0) = (4, 3)^T$, $x_3(0) = (2, 1)^T$, $x_4(0) = (0, -7)^T$, $x_5(0) = (-3, 3)^T$, $x_6(0) = (5, 0)^T$, and $v_1(0) = (-5, 2)^T$, $v_2(0) = (4, 3)^T$, $v_3(0) = (4, 3)^T$, $v_4(0) = (0, -7)^T$, $v_5(0) = (2, 1)^T$, $v_6(0) = (-2, 3)^T$. The nonlinear functions are defined as $h_1(t) = \frac{1}{10}\sin(x_1(t))$, $h_2(t) = \frac{1}{20}[\cos(x_2(t)) + \sin(v_2(t))]$, $h_3(t) = \frac{1}{10}\cos(v_3(t))$, $h_4(t) = \frac{1}{10}\sin(v_4(t))$, $h_5(t) = \frac{1}{10}\cos(x_5(t))$, and $h_6(t) = \frac{1}{10}\tanh(x_6(t))$. The sampling period is $h = 10^{-5}$, $\alpha(t) = \begin{cases} 75, t \in [2kh, h + 2kh), \\ 70, t \in [h + 2kh, 4kh), \end{cases}$ and $\beta(t) = \begin{cases} 70, t \in [2kh, h + 2kh), \\ 75, t \in [h + 2kh, 4kh), \end{cases}$ where $k \in \mathbb{Z}$. Furthermore, the parameters are set as $\sigma_1 = 10$, $\sigma_2 = 20$, $\sigma_3 = 10$, $\sigma_4 = 20$, and $\sigma_5 = 10$ in (23). The topologies of followers are considered under both connected and disconnected cases. The corresponding Laplacian matrices are given by

$$L_1 = \begin{bmatrix} 2 & -1 & 0 & -1 & 0 \\ -1 & 2 & 0 & 0 & -1 \\ 0 & 0 & 1 & 0 & -1 \\ -1 & 0 & 0 & 1 & 0 \\ 0 & -1 & -1 & 0 & 2 \end{bmatrix}, L_2 = \begin{bmatrix} 1 & 0 & 0 & -1 & 0 \\ 0 & 1 & -1 & 0 & 0 \\ 0 & -1 & 2 & 0 & -1 \\ -1 & 0 & 0 & 1 & 0 \\ 0 & 0 & -1 & 0 & 1 \end{bmatrix}.$$

L_1 and L_2 correspond to Figure 3 and Figure 4, respectively.

Moreover, the pinning strength matrices Υ_1 and Υ_2 are selected defined as follows, corresponding to Figure 3 and Figure 4, respectively. According to Remark 3, node 2 is selected as the pinning node with pinning gain

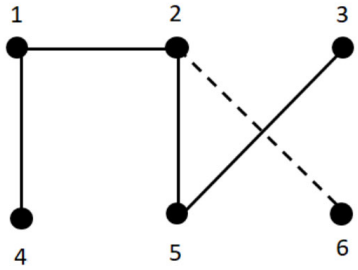


Figure 3. Second-order heterogeneous MASs over a connected graph.

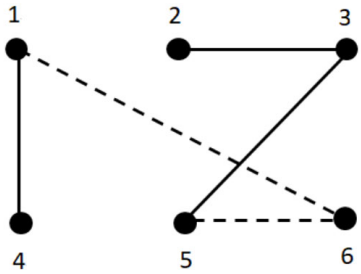


Figure 4. Second-order heterogeneous MASs over a disconnected graph.

$\varrho_2 = 1$ for Figure 3. Nodes 1 and 5 are selected as pinning nodes with gains $\varrho_1 = \varrho_5 = 2$ for Figure 4. Therefore, the Υ_1 and Υ_1 matrices are expressed as $\Upsilon_1 = \begin{bmatrix} 0 & 0 & 0 & 0 & 0 \\ 0 & 1 & 0 & 0 & 0 \\ 0 & 0 & 0 & 0 & 0 \\ 0 & 0 & 0 & 0 & 0 \\ 0 & 0 & 0 & 0 & 0 \end{bmatrix}$ and $\Upsilon_2 = \begin{bmatrix} 2 & 0 & 0 & 0 & 0 \\ 0 & 0 & 0 & 0 & 0 \\ 0 & 0 & 0 & 0 & 0 \\ 0 & 0 & 0 & 0 & 0 \\ 0 & 0 & 0 & 0 & 2 \end{bmatrix}$. It is calculated that $\max\{\zeta_1(t)\} = -0.2448$, $\max\{\zeta_2(t)\} = 0.1908$, and $\max\{\tilde{\zeta}_1(t)\} = -0.2001$ when $J = \frac{1}{10}\mathrm{I}_5$. Finally, the condition $C - J > 0$ must be verified. For the connected and disconnected graphs corresponding to Figures 3 and 4, C is given as $\begin{bmatrix} 28 & -14 & 0 & -14 & 0 \\ -14 & 42 & 0 & 0 & -14 \\ 0 & 0 & 14 & 0 & -14 \\ -14 & 0 & 0 & 14 & 0 \\ 0 & -14 & -14 & 0 & 28 \end{bmatrix}$ and $\begin{bmatrix} 42 & 0 & 0 & -14 & 0 \\ 0 & 14 & -14 & 0 & 0 \\ 0 & -14 & 28 & 0 & -14 \\ -14 & 0 & 0 & 14 & 0 \\ 0 & 0 & -14 & 0 & 42 \end{bmatrix}$, respectively. By simple calculation, it can be confirmed that $C - J$ is positive definite in both cases.

Example 1. *Lead-following consensus under time-driven sampling control*

In this example, consensus of systems (1)-(2) is simulated using controller (6), which does not include event-triggered control. Figures 5 and 6 show the consensus error trajectories of the position and velocity states of six nodes in a connected network. Correspondingly, Figures 7 and 8 sketch the consensus error trajectories for a disconnected network. As shown in Figures 5-8, the heterogeneous second-order MASs eventually achieve consensus.

In the following, the error trajectories of the position and velocity states of the nodes under the disconnected topology are presented. In a disconnected graph, the leader node needs to pin at least one node in each connected component to ensure that all nodes can achieve consensus. Under the same initial conditions in Example 1, a comparison between connected and disconnected graphs is conducted. The results show that consensus is achieved by all nodes at approximately $t = 4.5$.

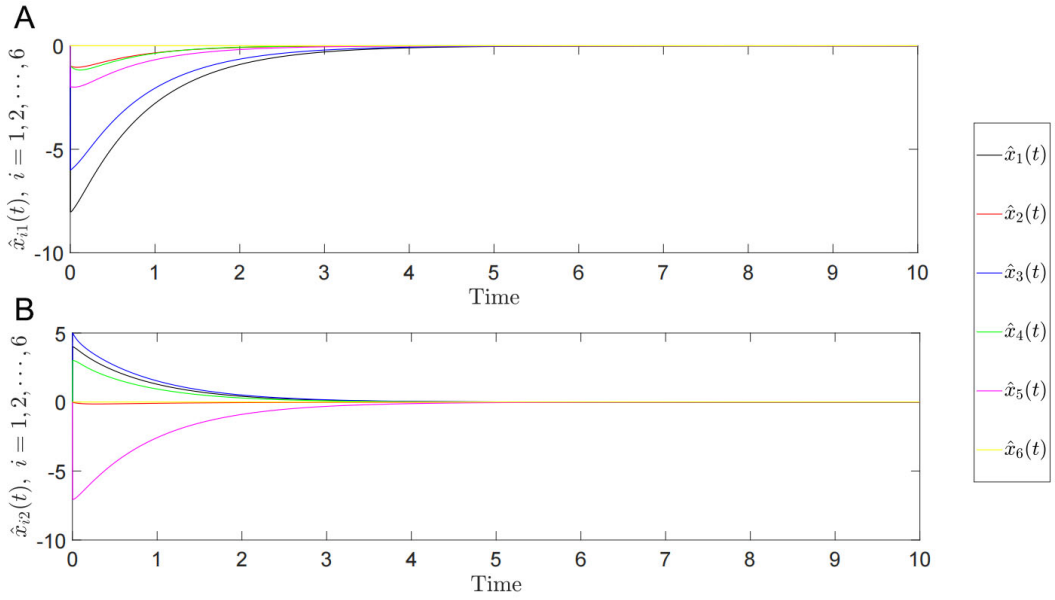


Figure 5. Error trajectories of (A) the first component and (B) the second component of the nodes' position over the connected graph.

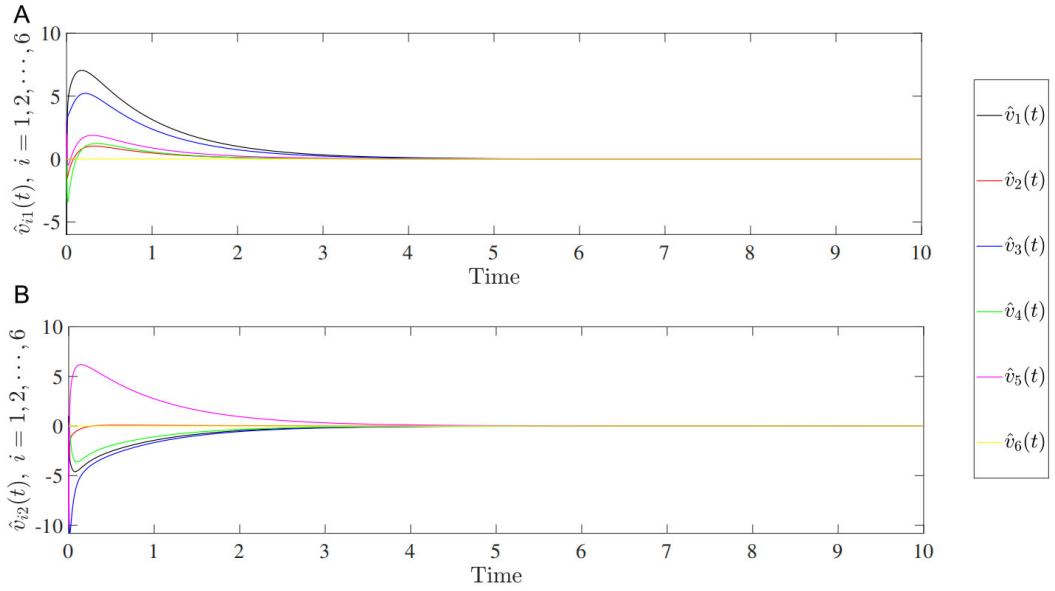


Figure 6. Error trajectories of (A) the first component and (B) the second component of the nodes' velocity over the connected graph.

Remark 8. *The sampling period h is a fundamental design parameter that significantly affects both the theoretical guarantees and the practical performance of the control system. Its role is twofold and closely integrated within the closed-loop dynamics. First, from a stability perspective, h is not merely an implementation constant but appears intrinsically within the sufficient conditions for consensus. In the subsequent Lyapunov analysis, the discretization errors introduced by the sampled-data control, such as $\hat{x}(t) - \hat{x}(lh)$, lead to terms in the derivative of the Lyapunov functional that scale linearly with h, such as terms proportional to $\alpha(t)h\|J(L+\Gamma)\|$. Consequently, the coefficients $\zeta_1(t)$ and $\zeta_2(t)$ in the core stability condition (8) of Theorem 1 become explicit functions of h. This establishes a direct theoretical link: increasing h tightens the stability condition, effectively imposing an upper bound on the*

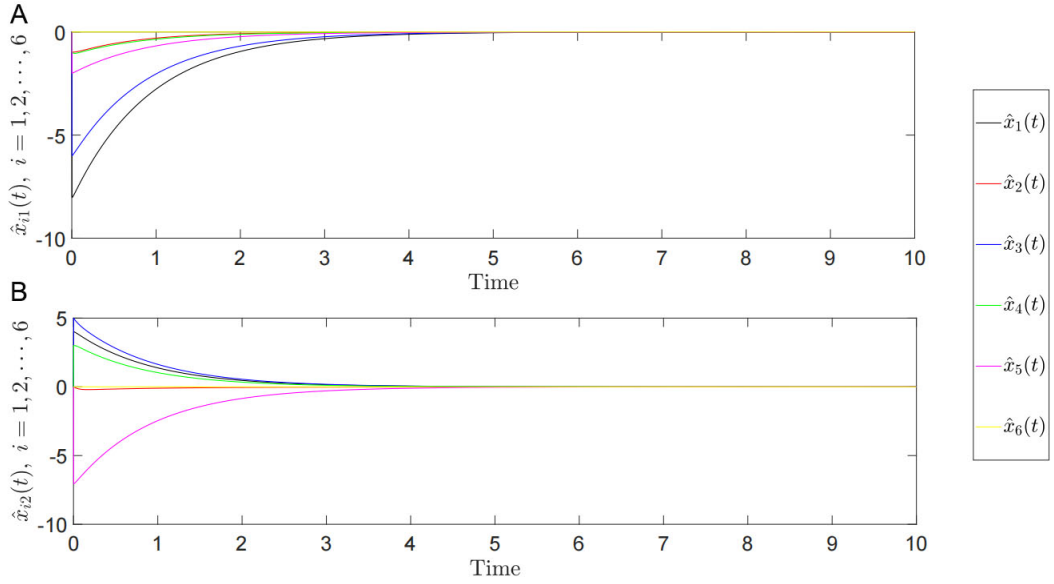


Figure 7. Error trajectories of (A) the first component and (B) the second component of the nodes' position over the disconnected graph.

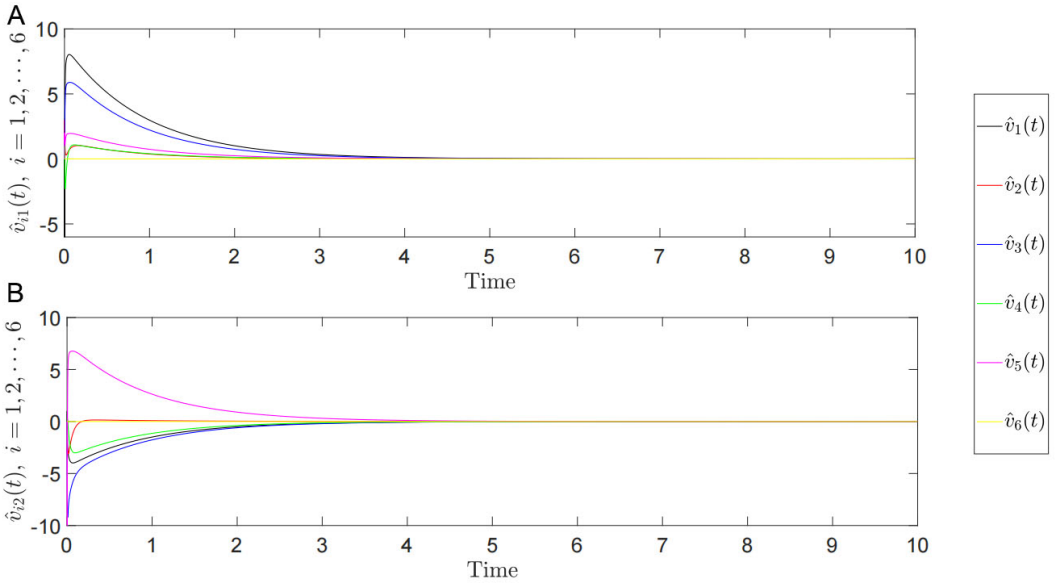


Figure 8. Error trajectories of (A) the first component and (B) the second component of the nodes' velocity over the disconnected graph.

allowable sampling period for provable exponential convergence. Second, from a resource utilization perspective, h defines the fundamental temporal resolution of the system. It dictates the fixed update interval of the pure sampling controller and, more importantly, sets the minimum possible inter-event time in the event-triggered strategy, thereby determining the maximum achievable communication frequency. Thus, the choice of h reflects an inherent trade-off between stability margin robustness (favored by a smaller h) and the inherent demand on communication and computational resources (favored by a larger h). The following analysis formally characterizes this dual dependence.

Example 2. *Lead-following consensus under event-triggered control*

In this example, the consensus of the systems (1) and (2) is simulated via the event-triggered control strategy (21).

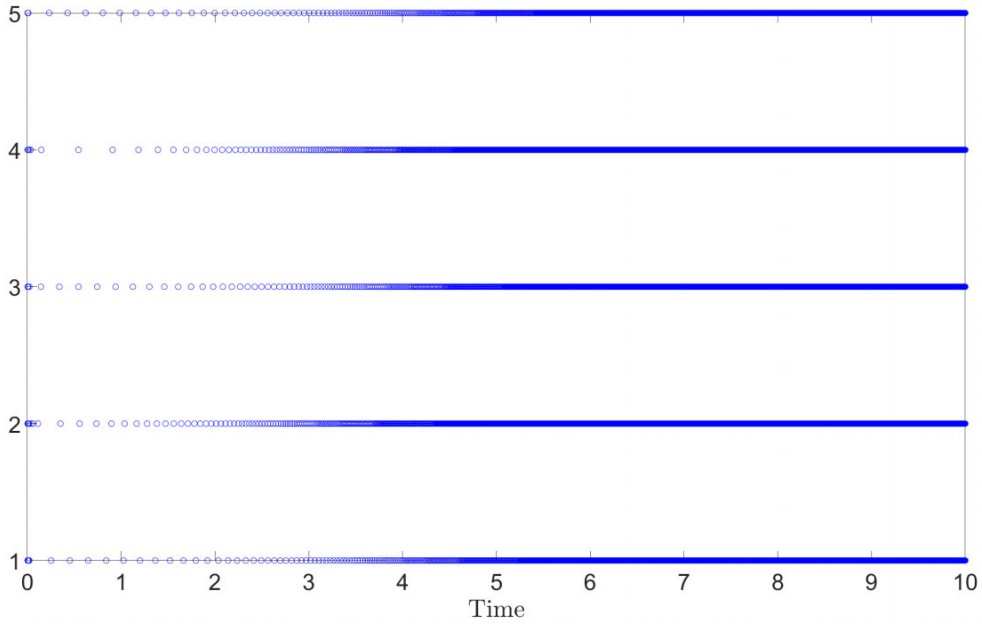


Figure 9. The triggering instants of control (21) over the connected graph.

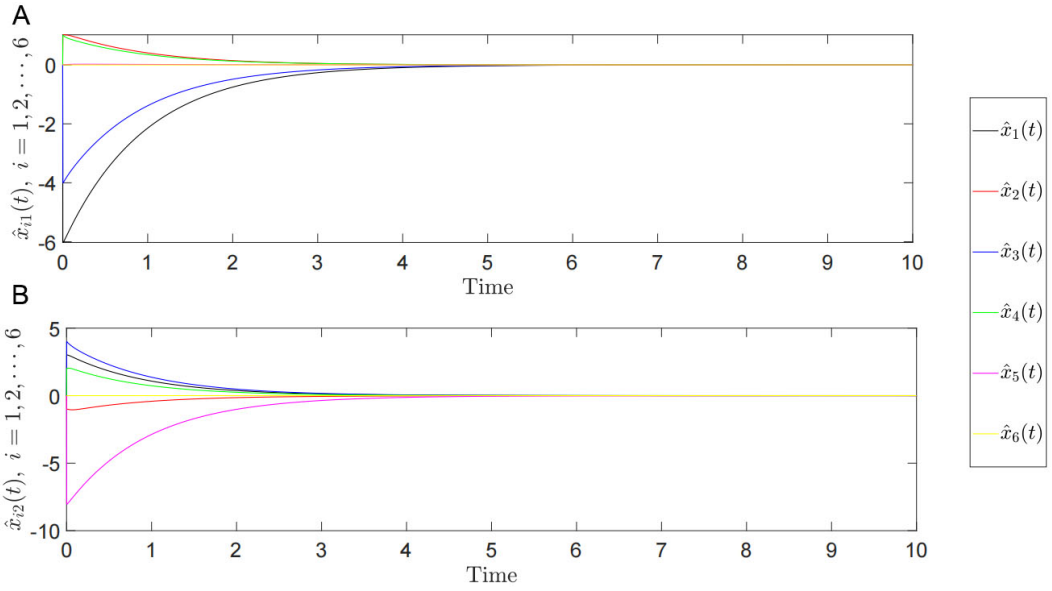


Figure 10. Error trajectories of (a) the first component and (b) the second component of the nodes' positions over the connected graph under control 21.

Figure 9 shows the triggering instants over the connected graph when the nodes in the MASs reach consensus. From Figure 9, it can be observed that the number of triggering instants evolves from sparse to dense, which is related to the designed triggering function (23). Moreover, Figures 10 and 11 show that the error trajectories of the MASs converge to consensus under the event-triggered mechanism. Correspondingly, Figures 12 and 13 present the consensus error trajectories under the event-triggered mechanism over the disconnected network. Figure 14 shows the triggering instants over the disconnected graph when the nodes in the MASs reach consensus.

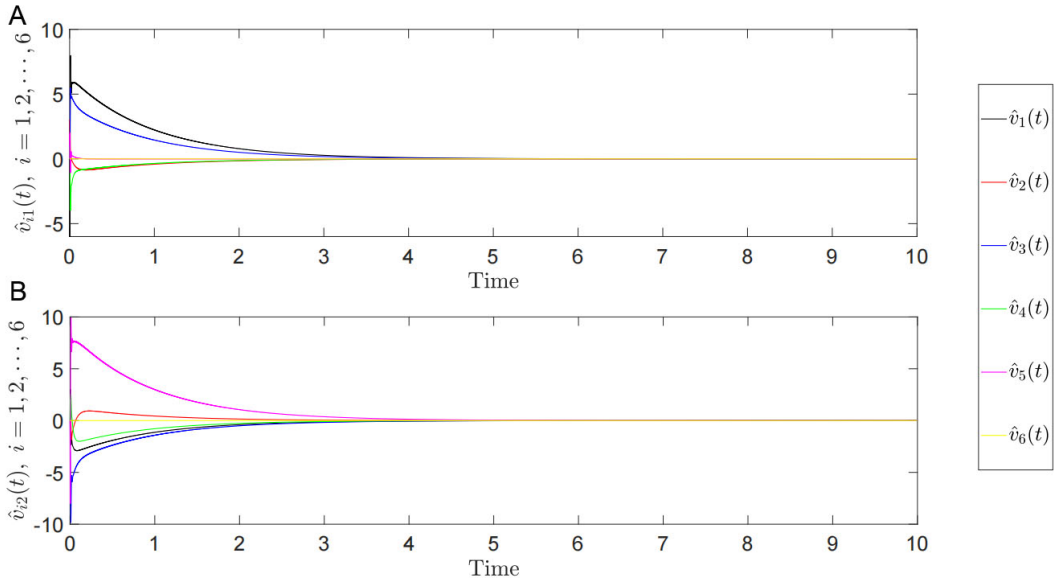


Figure 11. Error trajectories of (A) the first component and (B) the second component of the nodes' velocities over the connected graph under control 21.

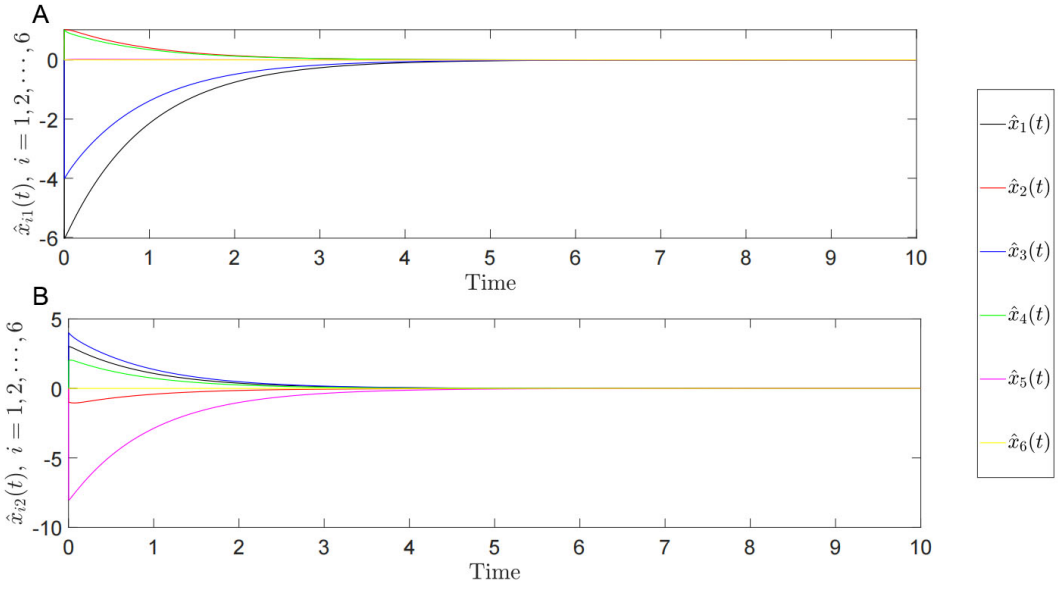


Figure 12. Error trajectories of (A) the first component and (B) the second component of the nodes' positions over the disconnected graph under control 21.

Remark 9. *It is worth noting from Figures 9 and 14 in this example that Zeno behavior does not occur, although the triggering becomes more frequent over time. Since sampling control is applied in both control schemes designed in this paper, and triggering instants are restricted to occur only at sampling instants, Zeno behavior can be naturally excluded.*

The difference between Example 1 and Example 2 is the error trajectories of each node under different controllers. The controller used in Example 1 is a sampling controller, whereas Example 2 employs a sampling-

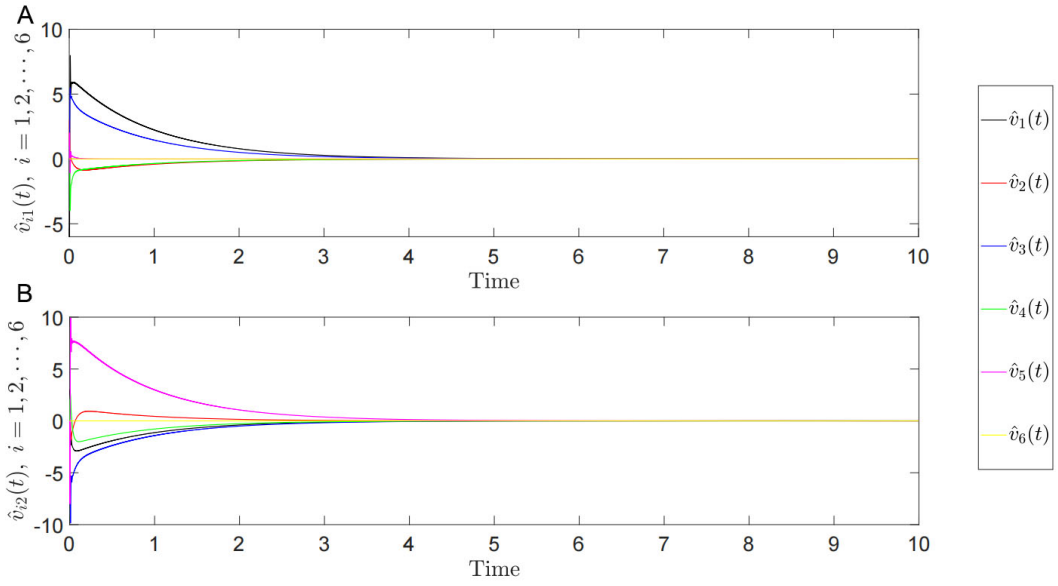


Figure 13. Error trajectories of (A) the first component and (B) the second component of the nodes' velocities over the disconnected graph under control 21.

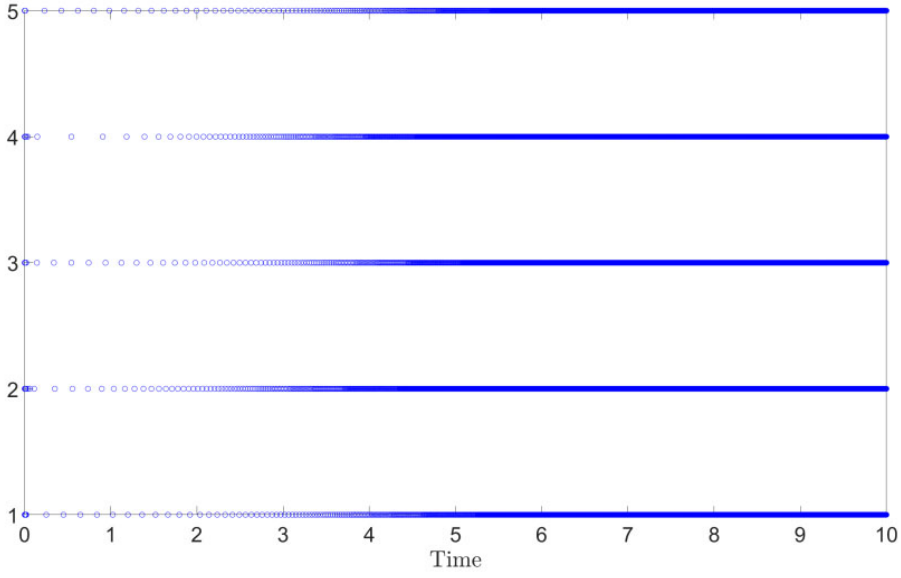


Figure 14. The triggering instants of control 21 over the disconnected graph.

based event-triggered control mechanism. The results shown in the above figures indicate that the nodes can achieve consensus under both controllers. In addition, the system considered in this paper is a heterogeneous MAS, meaning that the dynamics of each agent are different. As a result, achieving complete consensus is more challenging. In the numerical simulations, the consensus errors of the position and velocity states remain within a small upper bound , indicating that the heterogeneous MAS can still achieve satisfactory consensus.

Remark 10. *The controller in Theorem 2 extends the sampling-based controller in Theorem 1 by introducing an event-triggered mechanism, such that control updates are applied only at triggering instants, thereby reducing communication costs to some extent. The controller in this subsection is shown in (21). Since the consensus error*

eventually approaches zero, i.e., $\sigma_i(\|\hat{x}_i(t^i_{k_i}h+mh)\|^2+\|\hat{v}_i(t^i_{k_i}h+mh)\|^2)\to 0$ *when* $t\to\infty$*, the number of triggering instants evolves from sparse to dense. However, because triggering instants occur only at discrete sampling instants, Zeno behavior is naturally avoided.*

Remark 11. *Research on consensus in MASs remains an active and significant area, with various methodologies continuously being developed. For instance, literature*[20] *studied a consensus strategy for a novel nonlinear MAS under DoS attacks, employing a saturated impulsive control mechanism and analyzing stability via Lyapunov theory and matrix measure theory. Literature*[2] *proposed a robust non-fragile* H_∞ *filtering method for fuzzy fractional order systems, and addressed the* H_∞ *control problem based on linear matrix inequalities. Literature*[32] *investigated the* H_∞ *control problem for fractional-order neural networks under spoofing attacks using an improved memory-based event-triggered strategy. In contrast, the present work focuses on the consensus problem of heterogeneous second-order nonlinear MASs and proposes two distinct control strategies. Specifically, a time-driven sampling controller and an event-triggered controller are designed, both incorporating time-varying control gains. In addition, matrix theory is used to derive consensus criteria for heterogeneous second-order MASs under both sampling control and event-triggered control. Zeno behavior is naturally excluded because periodic sampling is included in the control strategy.*

5.CONCLUSION

This work investigates the consensus problem for heterogeneous second-order MASs. To ensure consensus, the consensus problem in MASs was transformed into a stability problem of the corresponding error system. Subsequently, sufficient criteria for achieving quasi-consensus were derived using stability theory. It is worth noting that two control protocols were designed in this study. The difference between the two control strategies lies in whether an event-triggered mechanism is incorporated. The second controller introduces an event-triggered mechanism based on the design of the first controller, which could further reduce control cost. In addition, Zeno behavior does not occur, as a sampling mechanism is applied in the control strategies. The minimum lower bound of the event-triggered intervals is equal to the sampling period. Finally, numerical examples were presented to validate the derived theoretical results. The current analysis assumes the absence of external disturbances. However, the quasi-consensus framework is inherently robust to bounded disturbances, as such disturbances can be regarded as additional bounded inputs in the error dynamics, leading to an increase in the ultimate error bound. Future work will explicitly incorporate and analyze the effects of persistent external disturbances and design corresponding disturbance rejection mechanisms. Furthermore, the study of fully distributed algorithms and security control[29] for second-order networked systems remains both challenging and important, and these topics will be investigated in future work.

DECLARATIONS

Authors' contributions

Made substantial contributions to the conception and design of the study and performed data analysis and interpretation: Sun, S.; Wang, Z.

Performed data acquisition, as well as providing administrative, technical, and material support: Huang, C.; Feng, Y.; Xiao, M.

Availability of data and materials

The original contributions presented in this study are included in the article. Further inquiries can be directed to the corresponding authors.

AI and AI-assisted tools statement

Not applicable.

Financial support and sponsorship

This work was supported in part by the National Natural Science Foundation of China(Grant Nos. 62476138 and 42375016) and in part by the Postgraduate Research and Practice Innovation Program of Jiangsu Province (Grant KYCX23_0957).

Conflicts of interest

All authors declared that there are no conflicts of interest.

Ethical approval and consent to participate

Not applicable.

Consent for publication

Not applicable

Copyright

© The Author(s) 2026.

REFERENCES

1. Li, S.; Liang, K.; He, W. Fully distributed event-triggered secure consensus of general linear multi-agent systems under sequential scaling attacks *ISA Trans.* **2022**, *127*, 146-55. DOI
2. Li, B.; Zhang, X.; Zhao, X. Robust nonfragile H_∞ ffltering for fuzzy fractional order systems with uncertainties. *Iran. J. Fuzzy Syst.* **2024**, *21*, 1-7. DOI
3. Huang, C.; Li, H.; Cao, J. A novel strategy of bifurcation control for a delayed fractional predator–prey model. *Appl. Math. Comput.* **2019**, *347*, 808-38. DOI
4. Parhami, P.; Fateh, M.; Rezvani, M. A comparison of deep neural network models for cluster cancer patients through somatic point mutations. *J. Ambient Intell. Human. Comput.* **2022**, *14*, 10883-98. DOI
5. Wang, X.; Taul, M. G.; Wu, H. Grid-synchronization stability of converter-based resources an overview. *IEEE Open J. Ind. Applicat.* **2020**, *1*, 115-34. DOI
6. Hsieh, C. H.; Chen, Y. M. Fault tolerant consensus with multi-agent systems for distributed coordinated control algorithm in the energy internet network. *J. Phys. Conf. Ser.* **2019**, *1267*, 012079. DOI
7. Chen, C.; Xie, K.; Lewis, F. L.; Xie, S.; Fierro, R. Adaptive synchronization of multi-agent systems with resilience to communication link faults. *Automatica* **2020**, *111*, 108636. DOI
8. Mishra, M.; Poddar, P.; Agrawal, R.; Chen,J.; Tokekar, P.; Sujit, P. B. Multi-agent deep reinforcement learning for persistent monitoring with sensing, communication, and localization constraints. *IEEE Trans. Autom. Sci. Eng.* **2025**, *22*, 2831-43. DOI
9. Yang, Y.; Da, K.; Zhu, Y. Consensus based target tracking against deception jamming in distributed radar networks. *IET Radar. Sonar Navi.* **2023**, *17*, 683-700. DOI
10. Nowzari, C.; Garcia, E.; Cortés, J. Event-triggered communication and control of networked systems for multi-agent consensus. *Automatica* **2019**, *105*, 1-27. DOI
11. Dong, G.; Li, H.; Ma, H.; Lu, R. Finite-time consensus tracking neural network FTC of multi-agent systems. *IEEE Trans. Neural Netw. Learn. Syst.* **2020**, *32*, 653-62. DOI
12. Zhang, L.; Li, Y.; Lou, J.; Lu, J. Bipartite asynchronous impulsive tracking consensus for multi-agent systems. *Front. Inform. Technol. Electron. Eng.* **2022**, *23*, 1522-32. DOI
13. Lu, L.; Han, T.; Xiao, B.; Yan, H. Distributed observer-based predefined-time consensus control for second-order multi-agent systems. *Circuits. Syst. Signal Process.* **2023**, *42*, 7099-116. DOI
14. Zhao, D.; Dong, T.; Hu, W. Event-triggered consensus of discrete time second-order multi-agent network. *Int. J. Control. Autom. Syst.* **2018**, *16*, 87-96. DOI
15. Meng, T.; Xie, Y.; Lin, Z. Consensus of second-order multi-agent systems under unknown but bounded measurement noises. *Syst. Control Lett.* **2019**, *133*, 104517. DOI
16. Yue, H.; Xia, J. Reinforcement learning-based optimal adaptive fuzzy control for nonlinear multi-agent systems with prescribed performance. *Complex Eng Syst.* **2023**, *3*, 19. DOI
17. Shi, Y.; Hu, J.; Wu, Y.; Ghosh, B. K. Intermittent output tracking control of heterogeneous multi-agent systems over wide-area clustered communication networks. *Nonlinear Anal. Hybrid Syst.* **2023**, *50*, 101387. DOI
18. Zhao, G.; Hua, C.; Liu, S. Sampled-data dynamic output feedback consensus control of multi-agent systems. *IEEE Trans. Network Sci. Eng.* **2022**, *9*, 3292-301. DOI

19. Yu, L.; Cui, Y.; Lu, Z.; Liu, Y. Sampled-based bipartite tracking consensus of nonlinear multiagents subject to input saturation. *Complex Eng. Syst.* **2022**, *2*, 6. DOI
20. Hu, X.; Xiong, Y.; Zhang, Z.; Li, C. Consensus of a novel heuristic nonlinear multi-agent system in DOS attack network environment via saturation impulse control mechanism. *ISA Trans.* **2021**, *19*, 200-8. DOI
21. Hao, L.; Zhan, X.; Wu, J.; Han, T.; Yan, H. Fixed-time group consensus of nonlinear multi-agent systems via pinning control. *Int. J. Control. Autom. Syst.* **2021**, *19*, 200-8. DOI
22. Guo, X.; Liu, P.; Wang, J.; Ahn, C. K. Event-triggered adaptive fault-tolerant pinning control for cluster consensus of heterogeneous nonlinear multi-agent systems under aperiodic DoS attacks. *IEEE Trans. Network Sci. Eng.* **2021**, *8*, 1941-56. DOI
23. Yang, Y.; Qian, Y. Event-trigger-based recursive sliding-mode dynamic surface containment control with nonlinear gains for nonlinear multi-agent systems. *Inf. Sci.* **2021**, *560*, 202-16. DOI
24. Li, X. M.; Zhou, Q.; Li, P.; Li, H.; Lu, R. Event-triggered consensus control for multi-agent systems against false data-injection attacks. *IEEE Trans. Cybern.* **2019**, *50*, 1856-66. DOI
25. Xiong, Y.; Li, Y.; Xiong, Z.; et al. Power-exponential and fixed-time consensus of conformable fractional-order quantum cellular neural networks via event-triggered control. *Phys. Scr.* **2024**, *99*, 065247. DOI
26. Wang, Z.; Gao, Y.; Liu, Y.; Wang, S.; Wu, L. Distributed dynamic event-triggered communication and control for multi-agent consensus: a hybrid system approach. *Inf. Sci.* **2022**, *618*, 191-208. DOI
27. Han, Z.; Tang, W. K. S.; Jia, Q. Event-triggered synchronization for nonlinear multi-agent systems with sampled data. *IEEE Trans. Circuits Syst. I* **2020**, *67*, 3553-61. DOI
28. Wang, Z.; Shi, S.; He, W.; Xiao, M.; Cao, J.; Gorbachev, S. Observer-based asynchronous event-triggered bipartite consensus of multi-agent systems under false data injection attacks. *IEEE Trans. Control Netw. Syst.* **2023**, *10*, 1603-15. DOI
29. Kchaou, M.; Tajudeen, M. H. M.; Ali, M. S.; Perumal, R.; Priya, B.; Thakur, G. K. Annular finite-time stability for IT2 fuzzy networked switched system via non-fragile AETS under multiple attacks: application to tank reactor chemical process model. *Expert Syst. Appl.* **2024**, *255*, 124552. DOI
30. Wen, L.; Yu, Y.; Wang, W. Generalized Halanay inequalities for dissipativity of Volterra functional differential equations. *J. Math. Anal. Appl.* **2008**, *347*, 169-78. DOI
31. Boyd, S.; El Ghaoui, L.; Feron, E. Linear matrix inequalities in system and control theory. SIAM Press; 1994. Available from: https://web.stanford.edu/~boyd/lmibook/lmibook.pdf [Last accessed on 17 Apr 2026]
32. Banu, K. A.; Aparna, T.; Tajudeen, M. M. H_∞ control for fractional order neural networks with uncertainties subject to deception attacks via improved memory-event-triggered scheme and its application. *Neural Networks.* **2025**, *184*, 107092. DOI

Disclaimer/Publisher's Note: All statements, opinions, and data contained in this publication are solely those of the individual author(s) and contributor(s) and do not necessarily reflect those of OAE and/or the editor(s). OAE and/or the editor(s) disclaim any responsibility for harm to persons or property resulting from the use of any ideas, methods, instructions, or products mentioned in the content.

© The Author(s) 2026. **Open Access** This article is licensed under a Creative Commons Attribution 4.0 International License (https://creativecommons.org/licenses/by/4.0/), which permits unrestricted use, sharing, adaptation, distribution and repro-duction in any medium or format, for any purpose, even commercially, as long as you give appropriate credit to the original author(s) and the source, provide a link to the Creative Commons license, and indicate if changes were made.